Localized hepatic lobular regeneration by central-vein–associated lineage-restricted progenitors

Jonathan M. Tsai[a,b], Pang Wei Koh[c,d], Ania Stefanska[e], Liujing Xing[a], Graham G. Walmsley[a], Nicolas Poux[a], Irving L. Weissman[a,b,f,1,2], and Yuval Rinkevich[e,1,2]

[a]Institute for Stem Cell Biology and Regenerative Medicine, Stanford University School of Medicine, Stanford, CA 94305; [b]Department of Developmental Biology, Stanford University School of Medicine, Stanford, CA 94305; [c]Department of Genetics, Stanford University School of Medicine, Stanford, CA 94305; [d]Department of Computer Science, Stanford University, Stanford, CA 94305; [e]Comprehensive Pneumology Center, Institute of Lung Biology and Disease, Helmholtz Zentrum München, 81377 Munich, Germany; and [f]Ludwig Center for Cancer Stem Cell Biology and Medicine, Stanford University, Stanford, CA 94305

Contributed by Irving L. Weissman, February 25, 2017 (sent for review November 28, 2016; reviewed by Juan Carlos Izpisua Belmonte, Tatiana Kisseleva, George K. Michalopoulos, and Stewart Sell)

The regeneration of organ morphology and function following tissue loss is critical to restore normal physiology, yet few cases are documented in mammalian postnatal life. Partial hepatectomy of the adult mammalian liver activates compensatory hepatocyte hypertrophy and cell division across remaining lobes, resulting in restitution of organ mass but with permanent alteration of architecture. Here, we identify a time window in early postnatal life wherein partial amputation culminates in a localized regeneration instead of global hypertrophy and proliferation. Quantifications of liver mass, enzymatic activity, and immunohistochemistry demonstrate that damaged lobes underwent multilineage regeneration, reforming a lobe often indistinguishable from undamaged ones. Clonal analysis during regeneration reveals local clonal expansions of hepatocyte stem/progenitors at injured sites that are lineage but not fate restricted. Tetrachimeric mice show clonal selection occurs during development with further selections following injury. Surviving progenitors associate mainly with central veins, in a pattern of selection different from that of normal development. These results illuminate a previously unknown program of liver regeneration after acute injury and allow for exploration of latent regenerative programs with potential applications to adult liver regeneration.

liver | stem cells | regeneration | hepatocyte | lineage-restricted progenitors

In the postnatal liver (1–3), removal of up to 70% of mass results in acute expansion of hepatocytes in remaining lobes to compensate for lost function (4). The classical mechanism is a global program, in which remaining hepatocytes in all lobes hypertrophy, leading to enlargement of cell size and increase in metabolic activity (5). These hepatocytes undergo limited, tightly regulated cell divisions, such that S phase is not always followed by M phase, often generating polyploid hepatocytes, which may later undergo cytokinesis. Lobes subjected to 30% hepatectomy rarely undergo cell division, and compensate primarily by hypertrophy (5). Although total mass and function are restored within 1–2 wk following 70% and 30% hepatectomies, the damaged liver does not regenerate morphology, and instead develops a fibrotic scar that lacks normal cellular composition, with permanent loss of the normal architecture. The absence of regeneration is especially apparent during chronic injury where limited cell divisions and hypertrophy are exhausted by repeated damage.

It has been suggested that bipotent hepatic/cholangiocyte stem/progenitor cells proliferate and differentiate when hepatocyte proliferation is exhausted, as is the case during chronic injury (6–9), although this is controversial (10). Periportal hepatic stem or progenitor cells have been described in response to chemical injury models (11–13). However, to our knowledge, no known progenitor regenerating morphology has been reported after acute damage.

Whereas studies of liver development and homeostasis have reported that SRY (sex determining region Y)-box 9 ($Sox9^+$), leucine-rich repeat-containing G protein coupled receptor 5 ($Lgr5^+$) and more recently Axin2 (14) mark liver stem or progenitor cells (15, 16), no extensive, unbiased, in vivo clonal analyses exist regarding clone frequency, size, shape, contributions, and landmark associations, of the liver after acute tissue loss. Whether the liver is able to regenerate structurally after acute injury is still a question. Whereas prospective isolation and transplantation characterized hematopoietic (17) and central nervous system (CNS) stem cells (18), recent advances (19, 20) in clonal analysis have been useful in organ systems where transplantation is more difficult to perform (21).

Here we use a surgical procedure in which up to 30% of the left lobe is removed to chart liver regeneration at previously underexplored stages, and compare it to accepted regeneration models. Our model presents a framework to explore the reemergence of latent regenerative programs with potential applications to adult liver regeneration.

Results

We developed an acute injury model (*SI Appendix*) that involves resection of 20–30% of the inferior portion of the left lobe of newborn (day 0.5) mice [denoted surgery day 0 (S0)]. Mice that underwent surgery on postnatal day 0 (S0) were analyzed at 7, 35, and 56 d postlobular hepatectomy [S0, day 7 of analysis (D7); S0, D35; and S0, D56], at which all lobes were isolated and analyzed for gross histology and mass. Seven days following surgery (S0, D7) the amputated left lobe weighed on average 20–30% less than age-matched controls. Amputated lobes 56 d following injury (S0, D56) showed

Significance

After partial hepatectomy, the adult mammalian liver regenerates through the mobilization of all hepatocytes characterized by a few cycles of cell division and subsequent hypertrophy with loss of global architecture. We have discovered a form of regeneration in the neonatal mouse liver, specific to the first week of life, where we observe numerous rounds of cell division and reconstitution of lobe architecture much like in amphibian limbs. This regenerative process is characterized by clonal expansion of select hepatocyte-specific stem or progenitors that localize to the central vein and is one of the first characterized instances of true mammalian regeneration.

Author contributions: J.M.T., I.L.W., and Y.R. designed research; J.M.T., A.S., L.X., G.G.W., N.P., and Y.R. performed research; J.M.T., I.L.W., and Y.R. contributed new reagents/analytic tools; J.M.T., P.W.K., I.L.W., and Y.R. analyzed data; and J.M.T., I.L.W., and Y.R. wrote the paper.

Reviewers: J.C.I.B., The Salk Institute; T.K., University of California, San Diego; G.K.M., University of Pittsburgh; and S.S., Center and Ordway Research Institute, New York State Health Department, Wadsworth Center.

The authors declare no conflict of interest.

[1]I.L.W. and Y.R. contributed equally to this work.

[2]To whom correspondence may be addressed. Email: irv@stanford.edu or yuval.rinkevich@helmholtz-muenchen.de.

This article contains supporting information online at www.pnas.org/lookup/suppl/doi:10.1073/pnas.1621361114/-/DCSupplemental.

www.pnas.org/cgi/doi/10.1073/pnas.1621361114

little gross morphological differences compared with age-matched uninjured lobes, regenerating global structure, by morphology and histology (Fig. 1*A*), and were nonfibrotic by trichrome stain (Fig. 1*B*). The final mass of injured lobes after 56 d was within a SD to uninjured left lobes (Fig. 2*A* and *SI Appendix*, Fig. S1), suggesting a localized regeneration response.

Left lobes resected at S7, S10, and S14 similarly weighed ∼20–30% less than controls at 7 d. However, these amputations rarely showed an increase in mass over time in proportion to adjacent uninjured lobes (Figs. 2*B* and 3*A* and *SI Appendix*, Fig. S1). Gross morphology after 56 d revealed abnormally shaped left lobes with scar formation and an identifiable area of amputation (Fig. 1 *C* and *D* and *SI Appendix*, Fig. S2). Histology (hematoxylin and eosin and trichrome staining) showed progressive loss of regeneration correlated with increased collagen deposition at the site of damage (Fig. 1*D*) and often exhibited "clover-like" lobular structures, the result of fusion of the left and median lobes that was accompanied by adhesions to bowel or peritoneum (*SI Appendix*, Fig. S2).

There was no significant difference in final masses of adjacent nondamaged lobes from S0, D56 mice compared with that of uninjured mice after 56 d (Fig. 2*A*), indicating that regeneration was confined to the injured lobe, without compensatory growth from adjacent lobes. A gradual increase in compensatory growth occurred after 1 wk (Fig. 2*B* and *SI Appendix*, Fig. S1). Compensation indices, defined as the ratio of right lobe mass to the injured or uninjured left lobe mass (Fig. 3*B*), were calculated. In uninjured mice, the right lobe is ∼80% of the left lobe by mass and has a compensation index of 0.8, (no compensation). The compensation index at S0, D56 was not significantly different from uninjured controls. However, compensation indices at S7, D56; S10, D56; and S14, D56 were significantly higher, indicating compensation is a mechanism of regeneration after 7 d.

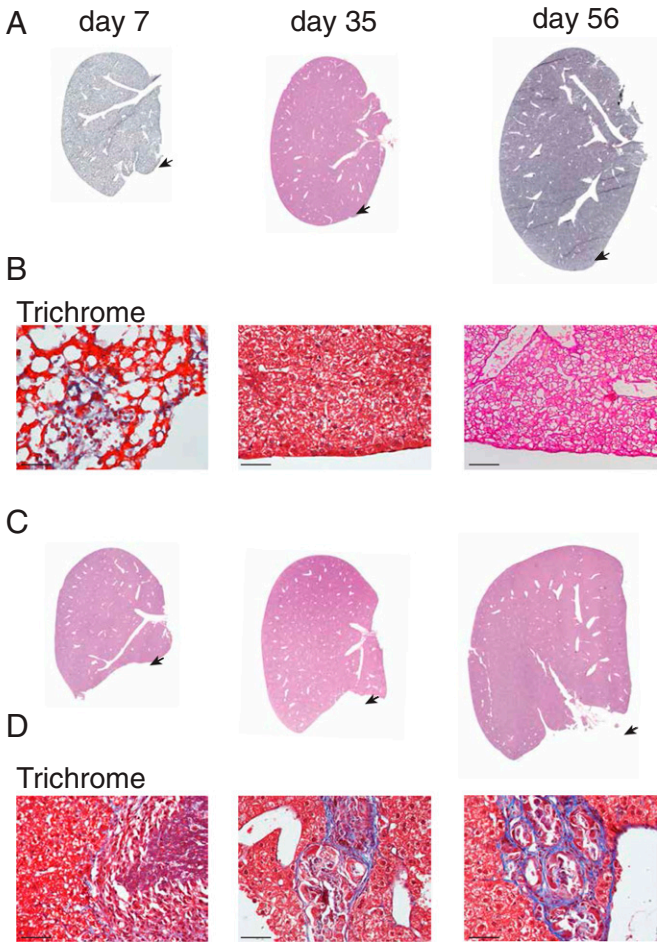

Fig. 1. Morphological regeneration of the left lobe occurs in neonatal mice. Hematoxylin and eosin (H&E) stains of the mouse liver at 7, 35, and 56 d post-resection from pups undergoing surgery on day 0 (*A*) or day 14 (*C*). Arrows denote area of amputation. Higher magnification of trichrome-stained sections focused on injury sites from day 0 mice undergoing surgery (*B*) and day 14 mice undergoing surgery (*D*) followed by 7, 35, and 56 d of recovery. (Scale bars, 50 μm.)

We found no difference in the distributions of hepatocytes (albumin$^+$), cholangiocytes (EpCAM$^+$), mesothelium (Podoplanin$^+$), and lymphatic ducts (Lyve-1$^+$) (*SI Appendix*, Fig. S3) in the regenerated lobe, indicating the main hepatic lineages are reconstituted. S0–S14 mice showed no signs of jaundice. Although hepatocytes share a common morphology, distinct subsets exist that differ by their expression of distinct suites of proteins (22–24). Immunohistochemistry of common liver enzymes glutamine synthetase (GS), carbamoyl phosphate synthase, (CPS) and cytochrome P450 2E1 (CP450) (*SI Appendix*, Fig. S4*A*) showed similar distributions to that of uninjured controls, suggesting that liver function has been restored. Estimations of single hepatocyte areas were compared across uninjured and injured lobes undergoing partial lobular hepatectomy (*SI Appendix*, Fig. S5*A*) and no difference between uninjured and amputated lobes (Fig. 3 *C* and *D*) was found, indicating negligible hypertrophy. The 5-ethynyl-2′-deoxyuridine (EdU) pulse-chase studies showed two to three times as many EdU$^+$ cells in the resected lobe compared with the same areas of uninjured controls (Fig. 3*E*) suggesting hepatocyte proliferation contributes to liver regeneration.

We performed clonal analysis of individual hepatocytes by using our "Rainbow" (*R26*$^{VT2/GK3}$), Cre-dependent reporter (25) that uses pairs of mutant LoxP sites to randomly recombine three of four fluorescent proteins (GFP, CFP, RFP, and OFP), resulting in each cell permanently expressing a single color (Fig. 4*A*). To analyze all cell types, including rare presumed multipotent stem cells, we used an unbiased lineage-tracing strategy independent of candidate markers by crossing Rainbow mice with mice harboring an inducible Cre–ERT2 fusion protein under the Actin promoter (*Actin*^{CreER}). Despite the chance of two adjacent cells sharing a similar color, we (25, 26) and others (20, 27) have reported that titration curves of low-dose tamoxifen administrations over extended periods of time uncovers a faithful readout comparable to those observed using tissue- or cell-specific reporters (21, 28).

Multiple sets of serial sections were taken randomly over the amputated and undamaged lobes and the numbers and peak sizes of clones were measured (Fig. 4*B* and *SI Appendix*, Fig. S6). Clones, defined as continuous clusters of cells with the same color, were significantly larger in the amputated lobe (some containing over 200 cells) compared with clones in the adjacent unamputated lobes of the same mouse (Fig. 4*B* and *SI Appendix*, Fig. S7). Most clones were found to be hepatocytes (albumin$^+$) compared with other liver markers (*SI Appendix*, Figs. S7 and S8). Comparable clone numbers (*SI Appendix*, Fig. S6) were found in injured, adjacent nondamaged lobes, and lobes from noninjured animals, suggesting a consistent rate of recombination. However, an increase in clone size was consistently documented in all regenerating lobes compared with clones from adjacent undamaged lobes or to control animals (*SI Appendix*, Figs. S9 and S10). This clonal bias hints at a subset of cells with a greater proliferative potential that our neonatal injury model activates specifically in the injured lobe.

Markedly different clonal behaviors and distributions were observed in control mice undergoing normal growth. We found similar hepatocyte clone sizes across all lobes (Fig. 4*C*), with the caudate lobe having a greater response. Mice undergoing 70% PHx were allowed to recover for 14 d, as previous studies showed no significant change in liver mass after 14 d recovery (4). The remaining enlarged liver lobes were isolated for clonal analysis. Clone sizes ranged between one and two cells, in agreement with established models (Fig. 4*D*) and these hepatocytes underwent

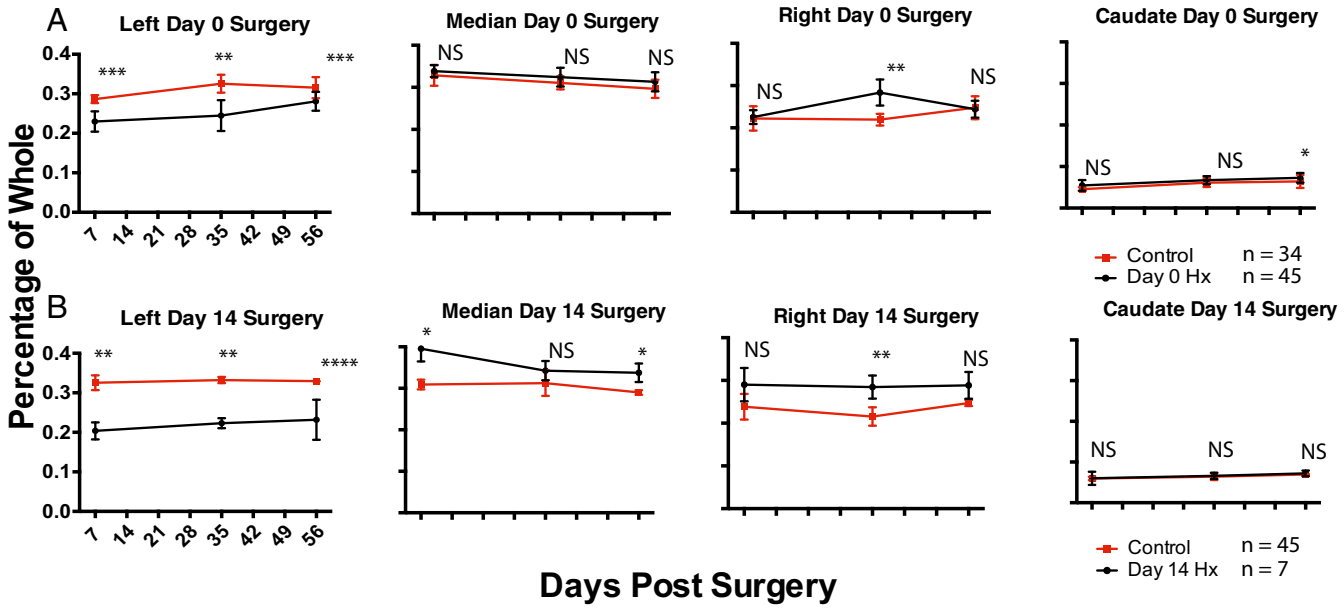

Fig. 2. Quantitative regeneration of the left lobe following partial lobular hepatectomy of P0 and P14 mice. The relative masses of all lobes are presented as percentage of whole liver mass after partial lobular hepatectomy of the left lobe at postnatal day 0 (*A*) or postnatal day 14 (*B*) after fixation plotted against recovery days postsurgery. The red line indicates uninjured age-matched controls. Values are presented as means ± SEM; $*P < 0.05$, $**P < 0.005$, $***P < 0.0005$; NS, not significant; $n = 5$ unless otherwise denoted. Quantitative assessment of the left lobe shows reconstitution of mass in pups undergoing surgery on day 0 (*A*) but not on day 14 (*B*). Values are presented as means ± SEM; $*P < 0.05$, $**P < 0.005$, $***P < 0.0005$; NS, not significant; $n = 5$ unless otherwise denoted.

hypertrophy as indicated by an increase in area over 14 d compared with controls (Fig. 3*C*).

We immunostained serial sections of $Actin^{CreERT2}R26^{VT2/GK3}$ regenerated lobes with CK18 and EpCAM, for overlapping expressions in single clones (Fig. 5*A*). We analyzed six fields across representative regions of each amputated left lobe and found in each region an average of 46 hepatocyte clones and an average of 9 bile duct clones (Fig. 5*B*). We found no clones with both markers. Clones of either fate in close proximity (Fig. 5*A*) never contributed to both populations, indicating lobe-specific regeneration is mediated by lineage-restricted progenitors (Fig. 5*C*); bipotent progenitors do not play a significant role. We

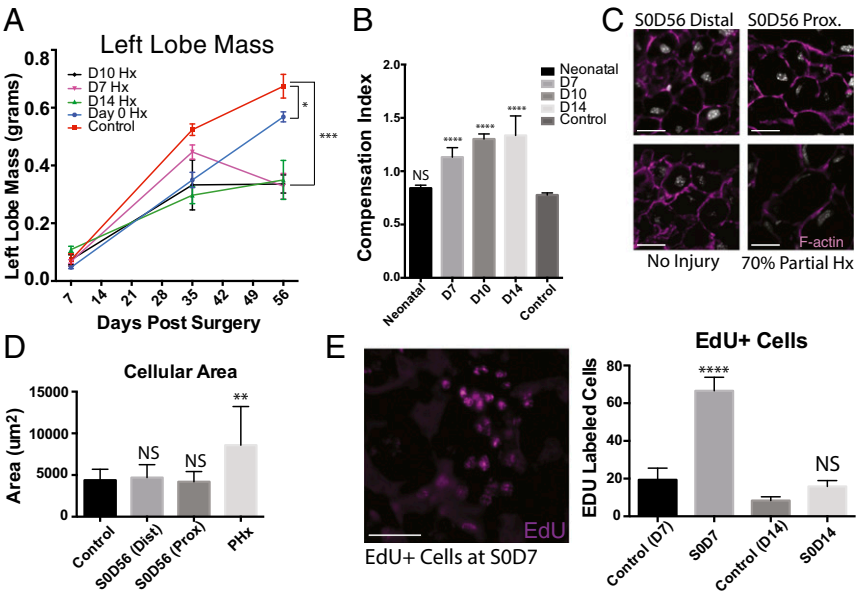

Fig. 3. Neonatal regeneration occurs through lobe-specific proliferation. (*A*) Reconstitution of left lobe mass across mice injured at D0, D7, D10, and D14 and uninjured mice. Values are means ± SEM; $***P < 0.0005$, $**P < 0.005$, $*P < 0.05$. (*B*) Compensation indices, expressed as the mass of the right lobe divided by the mass of the injured or uninjured left lobe is shown for uninjured mice and mice undergoing partial lobular hepatectomies at neonatal (P0) stages, postnatal days 7, 10, and 14 (D7, D10, and D14). (*C*) Representative images of sections from injured and left lobe 7 d after surgery (S0, D7) stained for filamentous actin and Hoechst 33342, $n = 48$. (*D*) Quantification of cell size estimated by area within actin membrane stains. Values are means ± SEM; NS, not significant; $**P < 0.005$, $n = 18$ for S0, D56 distal and proximal; control, $n = 6$ for S0, D14; $n = 6$ for adult 70% partial hepatectomy. (*E*) EdU^+ cells in the left lobe from day 0 mice undergoing partial lobular hepatectomy 7 d postsurgery. Quantification of EdU^+ cells is shown below. Values are means ± SEM. (Scale bars, 100 μm.)

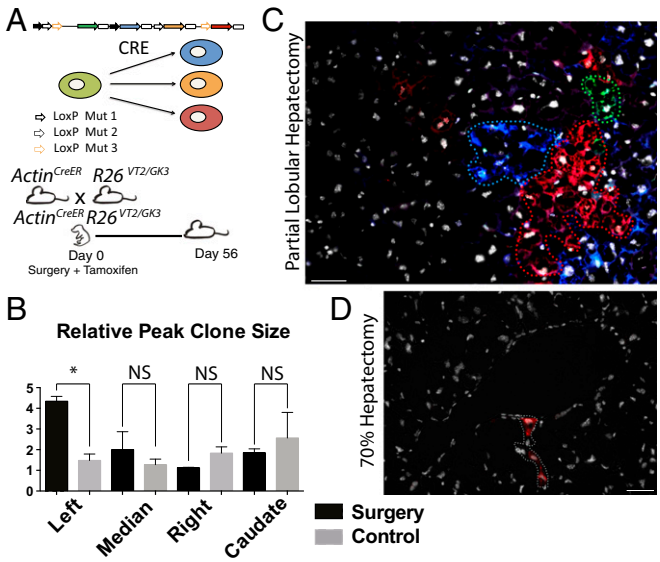

Fig. 4. The neonatal mouse liver regenerates through clonal hepatocyte proliferation. (*A*) Schematic of the Cre-dependent "Rainbow" reporter and experimental design: *Actin*^{CreERT2}*R26* $^{VT2/GK3}$ pups underwent partial lobular hepatectomy at day 0 and were treated with tamoxifen. Mice were followed for 56 d. (*B*) Analysis of relative peak clone size per lobe in mice 56 d post-surgery compared with age-matched controls. Values are means ± SEM; **P* = 0.05, ***P* < 0.005, ****P* < 0.0005, *n* = 1,445. Clones ranged from single cells to 408 (max). (*C*) Representative image across three channels (GFP, RFP, and CFP) showing large multicolor clones in a 56-d postpartial hepatectomy day 0.5 mouse merged with Hoechst 33342. (*D*) Representative image showing smaller clones in an adult undergoing classical partial hepatectomy merged with Hoechst 33342. (Scale bars, 100 μm.)

analyzed clones from our *Actin*^{CreERT2}*R26*$^{VT2/GK3}$ mice receiving partial lobular hepatectomy and costained for GS, CPS, and CP450. We observed single cells expressing either GS or CP450 within single clones (*SI Appendix*, Fig. S4*B*). This finding indicates stem/progenitors maintain lineage but not fate restriction, as they contribute to hepatocyte subsets with different enzymatic functions. Recent studies proposed Sox9$^+$ and Axin2$^+$ mark stem/progenitor cells in the liver (14, 15). Our clonal studies in *Sox9*^{CreERT2}*R26*$^{VT2/GK3}$ and *Axin2*^{CreERT2}*R26*$^{mT/mG}$ mice, showed little expansion of Axin2$^+$ or Sox9$^+$ hepatic cells, indicating that neither marks our progenitor population (*SI Appendix*, Fig. S11).

To place our findings in the context of development, we generated tetrachimeric mice (21, 25) by injecting four to five red, four to five blue, and four to five green mouse embryonic stem (mES) cells into wild-type uncolored blastocysts, which were then implanted into the uterus of uncolored mice. Each cell stably expresses a different fluorescent protein (GFP, CFP, and RFP), allowing us to perform clonal analysis and determine approximate numbers of labeled progenitors that contribute to developing and regenerating lobes.

We performed lobular partial hepatectomies on tetrachimeric P0 livers. In all tetrachimera lobes, extremely large clones (albumin$^+$ or HNF4A$^+$ cells of a single color) (*SI Appendix*, Fig. S12), containing up to ∼80,000 cells (*SI Appendix*, Figs. S13–S16) were observed. Large clones were followed through multiple serial sections, often spanning the entire length or width of a lobe. We observed similar clone sizes across all lobes in uninjured and injured mice, with little significant bias between lobes and injury states (Fig. 6*A*, *n* = 6), likely because large clone sizes in the tetrachimeric adult mask subtle changes that occur during activation of proliferative subsets.

To observe clonal compositions of developing lobes we analyzed tetrachimeric mice at postnatal day 0 (P0) and embryonic day 15 (e15). Clone sizes in tetrachimera e15 and P0 were smaller (Fig. 6*B*, *n* = 30 clones from three livers per condition) than in tetrachimeric adults. We calculated approximate total clone numbers (*SI Appendix*), and found a strikingly greater total clone number in e15 mice (13,000–17,000) compared with P0 (2,000–5,000) (Fig. 6*C*). Total clone number present in tetrachimeric S0, D56 and simply D56 controls were relatively equal to that of the D0 mice, with on average 650 clones giving rise to the left lobe, 550 to the median lobe, 400 to the right lobe, and 250 to the caudate lobe. These findings suggest clonal selection occurs between e15 and postnatal day 0.

During our analysis, we noticed that 228 of 229 clones in uninjured tetrachimera livers (*n* = 3), and all 271 clones in injured livers (*n* = 3), were adjacent to blood vessels. However, in e15 livers, (*n* = 3), 1,157 of 8,041 clones were associated with vasculature, (14.38%) (Fig. 6*D* and *SI Appendix*, Fig. S17). This observation suggests clones associated with vasculature maintain a selective advantage and are more likely to continue into the adult.

To determine whether hepatic progenitors exist near portal or central veins, we counted 20 random substantive clones (over 50 nuclei) per lobe across all lobes in adult uninjured (*n* = 3) and regenerating livers (*n* = 3) and identified whether they were associated with the portal vein (with adjacent EpCAM$^+$ bile ducts) or the central vein (with a ring of GS$^+$ hepatocytes) (Fig. 6*E*). Clones were roughly evenly distributed between portal and central veins in all lobes of control and injured mice, indicating no bias. Regenerating clones in injured left lobes in S0, D56 mice (Fig. 6*E*) showed a clear bias toward the central vein, corroborating recent lineage tracing studies (14), but not the portal vein. When we analyzed clones adjacent to the portal vein for potential inclusion of cholangiocytes, we saw very few bipotent clones. Of 118 bile ducts observed across five livers, only one clone was found to include both fates, despite the large clone sizes. Instead, most clones encompassing bile ducts were monoclonal or polyclonal for bile duct epithelium (*SI Appendix*, Fig. S18).

Discussion

The recovery of lobe mass, lineage reconstitutions, and clonal analysis establish that injured livers in day 0 mice regenerate

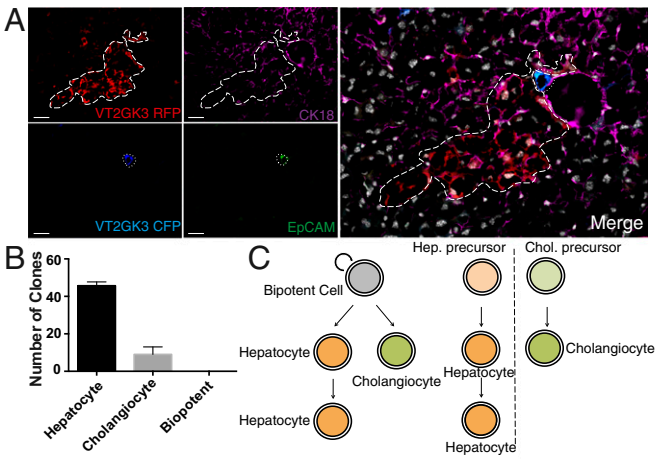

Fig. 5. Neonatal hepatic regeneration arises from lineage-restricted progenitors. S0, D56 livers from *Actin*^{CreERT2}*R26* $^{VT2/GK3}$ were sectioned and stained for CK18 and EpCAM to determine whether clones in the regenerated lobe contained both hepatocyte and bile duct epithelium. (*A*) Representative image of RFP and CFP clones overlaid with CK18 (Alexa Fluor 647) and EpCAM (Alexa Fluor 488); *n* = 164. (*B*) Clonal analysis (*n* = 164) across three S0, D56 *Actin*^{CreER}; *R26* $^{VT2/GK3}$ mice with hepatocyte, cholangiocyte, or both fates. (*C*) Proposed model of neonatal liver regeneration based on our data includes progenitors restricted to hepatic or cholangiocytic lineages. (Scale bars, 100 μm.)

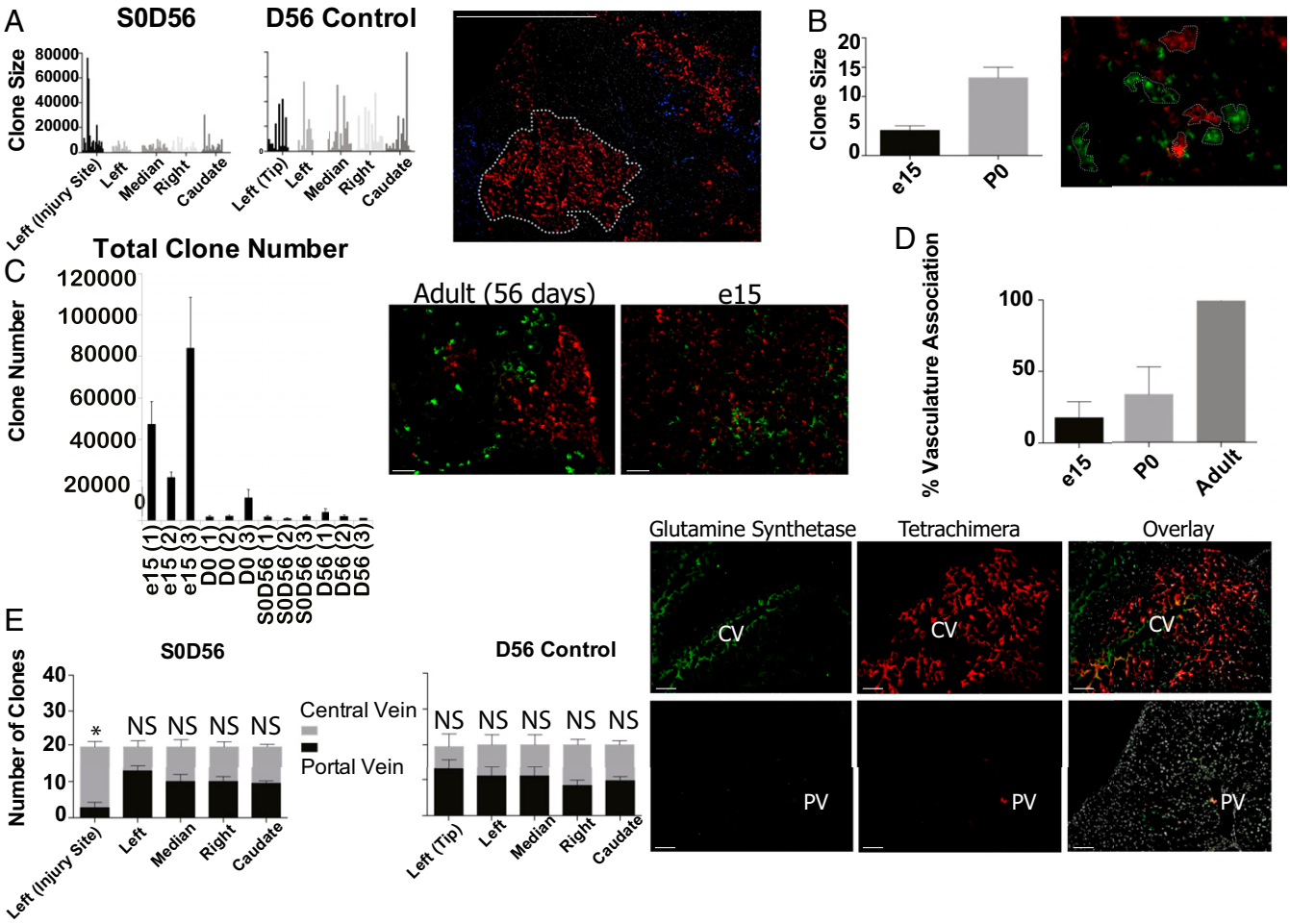

Fig. 6. Tetrachimeric analysis uncover expansions of pericentral-specific populations during regeneration. Tetrachimera pups underwent partial lobular hepatectomy at day 0 and were allowed to recover for 56 d. (*A*) Analyses of clone sizes in all lobes and the area of amputation in injured versus noninjured mice. Representative image of RFP and CFP tetrachimeric clones from the regenerating area is shown. (*B*) Clone sizes of embryonic day 15 (e15) tetrachimeric mice and day 0 tetrachimeric mice are significantly smaller than that of adult mice. Representative image of RFP and GFP tetrachimeric clones from the e15 liver is shown. (*C*) Approximate total clone number, measured by the clone density (number of clones per square millimeter) multiplied by total liver volume and corrected by the average depth of each clone, is higher in e15 tetrachimeric mice versus P0 and adult mice. Error bars are 90% confidence intervals. Representative images of RFP and GFP clones in adult (*Left*) and e15 (*Right*) tetrachimeric mice are shown. (*D*) e15, P0, and adult mice differ in the number of clones associated with vasculature. (*E*) Large clones in both regenerating and nonregenerating mice are associated equally with central and portal veins, except for those in the regenerating area of the left lobe. Representative image of clones associated with a central (*Top*) and portal (*Bottom*) vein. Central-vein–associated hepatocytes are stained with glutamine synthetase (GS^+). (Scale bars, 100 μm.)

predominantly by a new mechanism involving localized clonal expansions of hepatocytes, with little global compensation until after postnatal day 14. The classical view that a majority of postnatal liver hepatocytes have equal potential to contribute to functional regeneration after acute injury through limited divisions does not reflect what we observed. The infrequent, scattered distribution of hepatocyte clones and their nonuniform size indicates they arise from a subset of cells with higher regenerative potential instead of a homogenous population.

Regeneration in the liver has been reported alternately to be the result of transdifferentiation, or tissue specific stem cells, or hypertrophy (29). In organs that undergo continual homeostasis, such as the blood, regeneration is thought to result from multipotent stem cells that give rise to all lineages within that tissue (23, 24, 30). Our Rainbow lineage tracing data suggest that regeneration is the product of distinct hepatocyte and cholangiocyte restricted stem/progenitors and these lineage boundaries remain intact after tissue injury. This model mirrors similar findings in blood, the kidney (21), and digit tips (27).

Our Rainbow lineage tracing results argue against proliferation variability and stochastic division events. Large clones may be interpreted as variable proliferation rates; however, there is a consistent shift in clone sizes in our model. If proliferation variability were the only mechanism dictating clone size, a similar amount of clone sizes would be seen across all lobes (as observed in the control population). However, shifts in peak distributions to the injured left lobe argue for the mobilization of stem/progenitors. Though our data also do not preclude a population of bipotent cells either in development or regeneration, they play a minor role in this regenerative response. These multipotent progenitors are potentially elicited during chronic injury (31), but have little contribution during homeostasis and acute injury. Our tetrachimeric analysis indicates that a substantial number of progenitors seed the embryonic liver, but fewer remain and contribute to the adult, suggesting clonal selection. We have previously documented cases of stem cell competition (32, 33) and here, adult clones differ from fetal clones in vasculature association, suggesting this provides a selective advantage. The data indicate two potential progenitor pools give rise to the adult liver, associated with portal or central

veins. However, in our model, only the central-vein–associated pool is activated during this example of regeneration. This vascular association is reminiscent of recent findings that HoxB5$^+$ hematopoietic stem cells (HSCs) in mice are attached to venous sinusoidal endothelial cells (33). Regardless of the mechanism, our data show that the final clonal compositions of adult organs do not always reflect their original embryonic clonal makeup.

This work corroborates previous studies, which have suggested that a central-vein–associated Axin2$^+$ progenitor population contributes to homeostasis (14). Surprisingly, our Axin2 experiments yielded little clonal expansions, suggesting there may exist multiple progenitor populations. Other studies have implicated other factors such as Lgr5 (16), and Tbx3, though whether our population is distinct from these is yet to be determined (34). The identity of the putative stem/progenitors has yet to be characterized. We speculate this population could be similar to the adult liver stem cell or could be residual hepatoblasts found in the early postnatal liver. The latter is an attractive possibility (35, 36), as their loss in postnatal life correlates with our observed postnatal loss o regeneration.

Our model (Fig. 5*C*) raises important questions regarding the mechanisms that coordinate progenitors of different lineages to regenerate organized tissue. It is possible that damaged cells signal to progenitors to coordinate tissue reconstruction. To our knowledge, no system of communication between progenitors of different lineages has been well established. Therefore, our model may provide a framework to study the coordination between lineage-restricted precursors.

Recent studies have similarly shown neonatal regenerative potential in the first week of life in mouse digit tip and ear punch injuries (37), and in the heart (38). Whether this signifies a global response due to a soluble factor or independent mobilizations of tissue resident stem cells has yet to be investigated. Localized responses after partial hepatectomy have been reported, though the mechanism of our model requires further research (39, 40). Regardless, the identification of stages in which latent regenerative capacities exist is important to our understanding of mammalian regeneration and may lead to a therapeutic window in which transplanted progenitors may expand and regenerate function and structure.

Materials and Methods

All materials and methods can be found in *SI Appendix*, including those regarding partial lobular hepatectomy, 70% partial lobular hepatectomy, histology, clonal analysis, and lineage tracing. All animal experiments were carried out in strict accordance with the guidelines set forth by the Association for Assessment and Accreditation of Laboratory Animal Care International (AAALAC) and Stanford University's Administrative Panel on Laboratory Animal Care (APLAC), Protocol 12786, in the United States, or the European Animal Welfare Act, Directive 2010/63/EU.

ACKNOWLEDGMENTS. We thank C. Wang for generating tetrachimera mice; P. Chu for performing H&E and trichrome histology; and R. Nusse, J. Sage, P. Beachy, N. Fernhoff, R. Sinha, A. McCarty, J. P. Volkmer, A. Volkmer, K. Loh, B. Wang, D. Zhao, and K. Sylvester for helpful discussions. Research was supported by the Virginia and D. K. Ludwig Fund for Cancer Research; the National Heart, Lung, and Blood Institute (R01HL058770 and U01HL099999); and the California Institute for Regenerative Medicine (RC1 00354). Y.R. was supported by the Human Frontier Science Program Career Development Award (CDA00017), the German Research Foundation (RI 2787/1), the Siebel Stem Cell Institute, and the Thomas and Stacey Siebel Foundation (1119368-104-GHBJI). J.M.T. was supported by the NIH (T32GM007365), the National Research Service Award (1F30DK108561), and the Paul and Daisy Soros Fellowship for New Americans. Y.R. is a member of the German Center for Lung Research (DZL).

1. Michalopoulos GK (1997) Liver regeneration. *Science* 276(5309):60–66.
2. Ponfick VA (1890) Surgery of the liver. *Lancet* 1:881.
3. Higgins GAG (1931) Experimental pathology of the liver. Restoration of the liver of the white rat following partial surgical removal. *Arch Pathol (Chic)* 12:186–202.
4. Miyaoka Y, et al. (2012) Hypertrophy and unconventional cell division of hepatocytes underlie liver regeneration. *Curr Biol* 22(13):1166–1175.
5. Miyaoka Y, Miyajima A (2013) To divide or not to divide: Revisiting liver regeneration. *Cell Div* 8(1):8.
6. Sell S (2001) Heterogeneity and plasticity of hepatocyte lineage cells. *Hepatology* 33(3):738–750.
7. Wang X, et al. (2003) The origin and liver repopulating capacity of murine oval cells. *Proc Natl Acad Sci USA* 100(Suppl 1):11881–11888.
8. Fausto N (2004) Liver regeneration and repair: Hepatocytes, progenitor cells, and stem cells. *Hepatology* 39(6):1477–1487.
9. Shiojiri N, Lemire JM, Fausto N (1991) Cell lineages and oval cell progenitors in rat liver development. *Cancer Res* 51(10):2611–2620.
10. Yanger K, et al. (2014) Adult hepatocytes are generated by self-duplication rather than stem cell differentiation. *Cell Stem Cell* 15(3):340–349.
11. Rosenberg D, Ilic Z, Yin L, Sell S (2000) Proliferation of hepatic lineage cells of normal C57BL and interleukin-6 knockout mice after cocaine-induced periportal injury. *Hepatology* 31(4):948–955.
12. Yavorkovsky L, Lai E, Ilic Z, Sell S (1995) Participation of small intraportal stem cells in the restitutive response of the liver to periportal necrosis induced by allyl alcohol. *Hepatology* 21(6):1702–1712.
13. Sell S (1997) Electron microscopic identification of putative liver stem cells and intermediate hepatocytes following periportal necrosis induced in rats by allyl alcohol. *Stem Cells* 15(5):378–385.
14. Wang B, Zhao L, Fish M, Logan CY, Nusse R (2015) Self-renewing diploid Axin2(+) cells fuel homeostatic renewal of the liver. *Nature* 524(7564):180–185.
15. Furuyama K, et al. (2011) Continuous cell supply from a Sox9-expressing progenitor zone in adult liver, exocrine pancreas and intestine. *Nat Genet* 43(1):34–41.
16. Huch M, et al. (2013) In vitro expansion of single Lgr5+ liver stem cells induced by Wnt-driven regeneration. *Nature* 494(7436):247–250.
17. Spangrude GJ, Heimfeld S, Weissman IL (1988) Purification and characterization of mouse hematopoietic stem cells. *Science* 241(4861):58–62.
18. Uchida N, et al. (2000) Direct isolation of human central nervous system stem cells. *Proc Natl Acad Sci USA* 97(26):14720–14725.
19. Livet J, et al. (2007) Transgenic strategies for combinatorial expression of fluorescent proteins in the nervous system. *Nature* 450(7166):56–62.
20. Red-Horse K, Ueno H, Weissman IL, Krasnow MA (2010) Coronary arteries form by developmental reprogramming of venous cells. *Nature* 464(7288):549–553.
21. Rinkevich Y, et al. (2014) In vivo clonal analysis reveals lineage-restricted progenitor characteristics in mammalian kidney development, maintenance, and regeneration. *Cell Reports* 7(4):1270–1283.
22. Smith DD, Jr, Campbell JW (1988) Distribution of glutamine synthetase and carbamoylphosphate synthetase I in vertebrate liver. *Proc Natl Acad Sci USA* 85(1):160–164.
23. Schepers AG, et al. (2012) Lineage tracing reveals Lgr5+ stem cell activity in mouse intestinal adenomas. *Science* 337(6095):730–735.
24. Sato T, et al. (2009) Single Lgr5 stem cells build crypt-villus structures in vitro without a mesenchymal niche. *Nature* 459(7244):262–265.
25. Ueno H, Weissman IL (2006) Clonal analysis of mouse development reveals a polyclonal origin for yolk sac blood islands. *Dev Cell* 11(4):519–533.
26. Ueno H, Turnbull BB, Weissman IL (2009) Two-step oligoclonal development of male germ cells. *Proc Natl Acad Sci USA* 106(1):175–180.
27. Rinkevich Y, Lindau P, Ueno H, Longaker MT, Weissman IL (2011) Germ-layer and lineage-restricted stem/progenitors regenerate the mouse digit tip. *Nature* 476(7361):409–413.
28. Bonaguidi MA, et al. (2011) In vivo clonal analysis reveals self-renewing and multipotent adult neural stem cell characteristics. *Cell* 145(7):1142–1155.
29. Michalopoulos GK (2014) The liver is a peculiar organ when it comes to stem cells. *Am J Pathol* 184(5):1263–1267.
30. Barker N, et al. (2007) Identification of stem cells in small intestine and colon by marker gene Lgr5. *Nature* 449(7165):1003–1007.
31. Yimlamai D, et al. (2014) Hippo pathway activity influences liver cell fate. *Cell* 157(6):1324–1338.
32. Stoner DS, Rinkevich B, Weissman IL (1999) Heritable germ and somatic cell lineage competitions in chimeric colonial protochordates. *Proc Natl Acad Sci USA* 96(16):9148–9153.
33. Weissman IL (2015) Stem cells are units of natural selection for tissue formation, for germline development, and in cancer development. *Proc Natl Acad Sci USA* 112(29):8922–8928.
34. Chen JY, et al. (2016) Hoxb5 marks long-term haematopoietic stem cells and reveals a homogenous perivascular niche. *Nature* 530(7589):223–227.
35. Suzuki A, Sekiya S, Büscher D, Izpisúa Belmonte JC, Taniguchi H (2008) Tbx3 controls the fate of hepatic progenitor cells in liver development by suppressing p19ARF expression. *Development* 135(9):1589–1595.
36. Zaret KS, Grompe M (2008) Generation and regeneration of cells of the liver and pancreas. *Science* 322(5907):1490–1494.
37. Shyh-Chang N, et al. (2013) Lin28 enhances tissue repair by reprogramming cellular metabolism. *Cell* 155(4):778–792.
38. Porrello ER, et al. (2011) Transient regenerative potential of the neonatal mouse heart. *Science* 331(6020):1078–1080.
39. Kan NG, Junghans D, Izpisua Belmonte JC (2009) Compensatory growth mechanisms regulated by BMP and FGF signaling mediate liver regeneration in zebrafish after partial hepatectomy. *FASEB J* 23(10):3516–3525.
40. Paranjpe S, et al. (2016) Combined systemic elimination of MET and epidermal growth factor receptor signaling completely abolishes liver regeneration and leads to liver decompensation. *Hepatology* 64(5):1711–1724.